IEEE Photonics Journal
An IEEE Photonics Society Publication

Optimizing Plasmonic Grating Sensors for Limit of Detection Based on a Cramer–Rao Bound

Volume 2, Number 4, August 2010

Salman Karbasivalashani
Arash Mafi, Member, IEEE

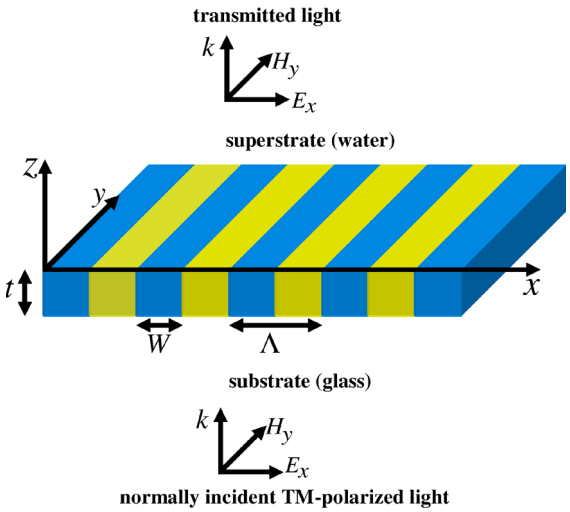

DOI: 10.1109/JPHOT.2010.2050874
1943-0655/$26.00 ©2010 IEEE

Optimizing Plasmonic Grating Sensors for Limit of Detection Based on a Cramer–Rao Bound

Salman Karbasivalashani and Arash Mafi, *Member, IEEE*

Department of Electrical Engineering and Computer Science,
University of Wisconsin–Milwaukee, Milwaukee, WI 53211 USA

DOI: 10.1109/JPHOT.2010.2050874
1943-0655/$26.00 ©2010 IEEE

Manuscript received April 26, 2010; revised May 14, 2010; accepted May 16, 2010. Date of publication May 20, 2010; date of current version June 18, 2010. This work was supported by the UWM Research Foundation's Catalyst Grant Program in Advanced Automation, made possible by support from the Rockwell Automation Charitable Corporation. Corresponding author: S. Karbasivalashani (e-mail: karbasi2@uwm.edu).

Abstract: We explore the impact of the geometrical features such as the period, duty cycle, and thickness on the performance of a metal-dielectric plasmonic grating sensor. The sensor is designed to operate at the wavelength of 850 nm for water-monitoring applications. Limit of detection (LOD) is chosen as the performance metric for the optimization of the sensor design. The LOD metric is based on a Cramer–Rao bound (CRB) and offers a theoretical lower limit on the estimation uncertainty of the spectral shift in the proposed sensor. We show that the lowest values of LOD correspond to grating designs, which result in step-like spectral features. An optimum grating design corresponds to gold stripes that are 160 nm thick and 456 nm wide on glass where the stripes are separated by 74 nm. Although our study is focused on a particular design and application, our methods and observations are applicable to a wide range of plasmonic grating sensor designs.

Index Terms: Plasmonics, sensors, gratings.

1. Introduction

Metal-dielectric plasmonic gratings have recently been the subject of many theoretical and experimental investigations. It has been shown that the excitation of surface plasmon resonance (SPR) waves can enhance the optical transmission through the grating structure resulting in highly peaked or large-slope spectral transmission features [1], [2]. A change in the refractive index of the surrounding medium can shift the wavelength location of these features, and the detection of such spectral shifts is used in label independent sensing. The geometry of diffractive gratings makes them appealing in applications where a small device footprint is desired, such as in highly integrated sensor systems. The possibility of high packing density and a large number of parallel channels with minimal analyte volume are other advantages of plasmonic grating sensors. Moreover, unlike prism-based plasmonic sensors, diffractive gratings do not require precision free-space optic alignment.

In this paper, we analyze and design a plasmonic grating sensor which operates at the wavelength of 850 nm for water-monitoring applications. We explore the impact of the geometrical features such as the period, duty cycle, and thickness on the performance of the proposed gold-dielectric plasmonic grating sensor. Limit of detection (LOD) is chosen as the performance metric for the optimization of the sensor design. The LOD metric is based on a Cramer–Rao bound (CRB) and offers a theoretical lower limit on the estimation uncertainty of the spectral shift in the proposed

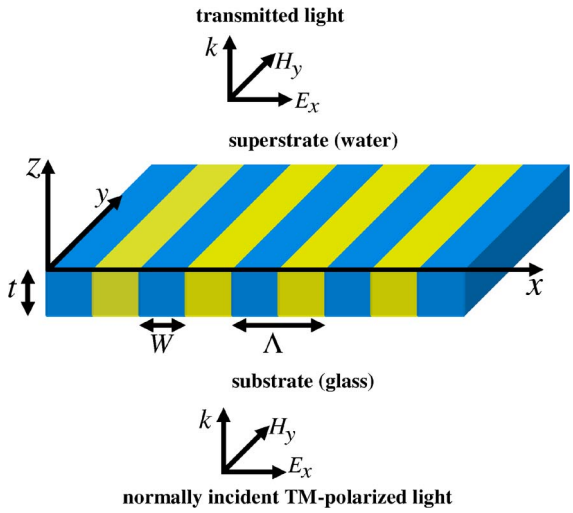

Fig. 1. Gold-dielectric grating structure.

sensor. We show that the lowest values of LOD correspond to grating designs, which result in step-like spectral features that are not in the conventional sharp and narrow spectral peaks.

There have already been several studies on the geometrical optimization of plasmonic grating structures. For example, the effect of the thickness on enhanced transmission spectrum of the gold-dielectric gratings has been addressed in [3] and [4]. Here, we study the impact of the period and duty cycle, in addition to the thickness. Our comprehensive study establishes general guidelines for achieving a desired transmission spectrum by engineering the geometry of the plasmonic grating. In order to perform a fair comparison of the performance among different grating structures, we choose to fix the peak wavelength of the transmission spectrum at 850 nm throughout our studies. The reason is that the choice of the sensing wavelength is often dictated by the specific application. In addition, the quality and the cost of sources and detectors vary significantly across the spectrum. A global optimization that also includes wavelength variation can result in an unnecessary wavelength-dependent bias, since the dielectric permittivity of gold varies significantly from visible to infrared. Taking these points into consideration and our desire for an optimized low-cost sensor for water monitoring led us to limit our studies to near 850 nm wavelength. We will present comparisons of the performance of the plasmonic grating sensors at different wavelengths in future work.

2. Structural Features and Its Impacts on Transmission Spectrum

The transmission spectrum of the grating structure in Fig. 1 depends on both the material and structural properties of the grating. In this paper, we focus on the design of a plasmonic grating for water-monitoring applications. We assume gold stripes are placed on a glass substrate with refractive index of 1.5 and that the superstrate is considered to be water (measurand or analyte) with refractive index of 1.3. We also assume that the gaps between gold stripes are filled with the measurand. The structural parameters for the metal-dielectric grating are period (Λ), duty cycle (ρ), and thickness (t) of the metal film. Duty cycle (ρ) is defined as the ratio of the dielectric material width (W), between gold stripes, to the period of the structure. We vary these structural parameters to study their impact on the transmission spectrum of the plasmonic grating and optimize the LOD of the sensor structure. The transmission spectrum is obtained using a commercial finite element method (FEM) software [5] and verified independently by an in-house developed FEM software [6], as well as an in-house developed rigorous coupled wave analysis (RCWA) code [7]. Periodic boundary conditions are implemented in FEM code to simulate the gold-dielectric grating. To model semi-infinite sub- or superstrate, perfectly matched layers (PMLs) are implemented in sub- and superstrate regions. In our simulations, we checked that the results are in the FEM convergence

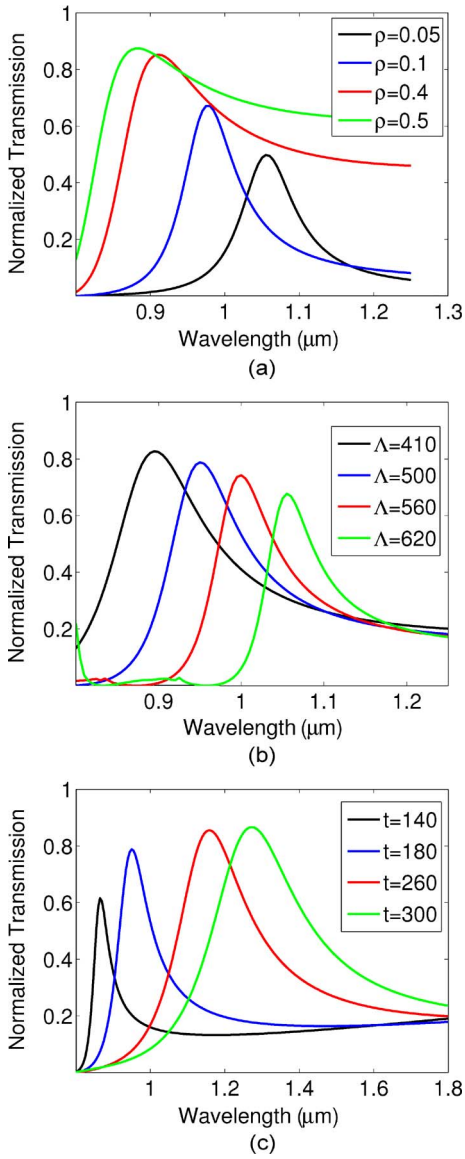

Fig. 2. Normalized transmission spectrum for a change in (a) duty cycle for $t = 180$ nm and $\Lambda = 500$ nm, (b) period for $t = 180$ nm and $\rho = 0.2$, and (c) thickness for $\rho = 0.2$ and $\Lambda = 500$ nm.

region. Most of our optimizations were done by using more than 500 000 mesh elements in each run, which was more than adequate for our simulations. We used a step size in wavelength of 0.5 nm to locate the transmission peaks. Gold permittivity is taken from the widely used experimental data of Johnson and Christy [8].

In this paper, we concentrate on wavelength interrogated sensors. To excite surface plasmons on the grating structure, TM-polarized light is assumed to be normally incident from the glass side (substrate) on the metal structure.

In order to isolate the impact of each grating structural parameter on the transmission spectrum, we vary the parameter while keeping the other two parameters fixed. In Fig. 2(a), we fix $t = 180$ nm and $\Lambda = 500$ nm and vary the duty cycle ρ. In Fig. 2(b), we fix $t = 180$ nm and $\rho = 0.2$ and vary the period Λ. In Fig. 2(c), we fix $\rho = 0.2$ and $\Lambda = 500$ nm and vary the thickness t. The impact of each structural parameter on the normalized enhanced transmission spectrum is clearly shown in these figures. We define the normalized transmission as the ratio of the transmitted power to the incident power over

each grating period at each wavelength. In particular, the resonance wavelength, i.e., the wavelength at which the transmission is maximally enhanced, and the peak value of the transmission are considerably affected by the structural parameters.

The peak transmission amplitude increases monotonically with the duty cycle: The duty cycle (ρ) is the ratio of the width of the dielectric material (W) to the period (Λ); therefore, a larger value of the duty cycle is equivalent to a smaller portion of the reflecting metal in the grating. However, increasing the duty cycle results in a blue-shift of the resonance wavelength, as shown in Fig. 2(a). The peak transmission amplitude decreases with increasing the period, as shown in Fig. 2(b). However, the resonance wavelength increases almost linearly with the period. This behavior can be explained by considering the fact that the resonance transmission wavelength λ_P of a plasmonic grating is roughly given by [9]

$$m\lambda_P = \Lambda\sqrt{\frac{\epsilon_D\epsilon_G}{\epsilon_D + \epsilon_G}}, \qquad m = 1, 2, \ldots \tag{1}$$

where ϵ_G is the effective grating permittivity, and ϵ_D is the permittivity, of the dielectric sub- or superstrate: λ_P is proportional to Λ.

The peak transmission amplitude increases with increasing the thickness as shown in Fig. 2(c). Increasing the grating thickness results in a red-shift of the resonance wavelength. Transmission resonances on metallic gratings with narrow slits are contributed [3] to the coupled surface plasmons and waveguide resonances. Since, for all designed gratings in this paper, the wavelength of the incident light is higher than the period (Λ), the enhanced transmission resonances can be provided by waveguide resonances.

Guided by the information from the above analysis, we can control and customize the properties of the transmission spectrum through the plasmonic grating structure. In the next section, we design and optimize a plasmonic sensor by varying the structural parameters of the grating based on the above guidelines.

3. Design of a Plasmonic Grating Sensor for Water-Monitoring Applications

In order to design and optimize a plasmonic grating sensor, we need to identify an appropriate metric. The most commonly applied metric in the optimization of wavelength interrogated systems is the sensitivity $s_\lambda = \partial\lambda_P/\partial n$. The sensitivity s_λ is evaluated at the peak transmission wavelength λ_P and measures the amount of the shift in the peak wavelength per unit change in the refractive index of the measurand: the superstrate water in our case. Although this metric is applied widely in the optimization of plasmonic sensors, it has serious deficiencies, for example, it is solely based on the location of the transmission peak and ignores the impact of the shape of the spectral feature. Intuitively, it is clear that even for identical values of s_λ, it is easier to detect a shift in a tall narrow spectral feature compared with a short and wide one. In addition, for our plasmonic grating sensor, $s_\lambda \approx 450$ (nm/RIU) and does not vary appreciably over the design space. The effect of a change in the refractive index of superstrate on the normalized enhanced transmission spectra for a set of engineered structural parameters is shown in Fig. 3. Full width at half maximum (FWHM) is another metric that can be applied in the optimization of these sensors. However, FWHM only incorporates the impact of the shape of the transmission spectrum to the first order and ignores higher order effects, such as the strong asymmetry of the Lorentzian-like transmission peaks. We argue that the appropriate metric for the optimization of our plasmonic sensor is the LOD, which is based on the CRB that determines the theoretical lower-bound on the estimation uncertainty of the spectral shift.

This metric, which fully incorporates the impact of the spectral shape, has been recently applied in the optimization of prism-based plasmonic sensors [10]. We will apply the LOD metric in the design of the plasmonic grating sensor and vary the three structural parameters ρ, Λ, and t to optimize the performance of the sensor. We also choose to fix the resonance wavelength at $\lambda_P = 850$ nm by tailoring the structural parameters. The rational behind this choice is the availability of low cost high quality optical sources and detectors at this wavelength. In addition, this constraint allows us to conduct a fair comparison among various designs in our optimization procedure without

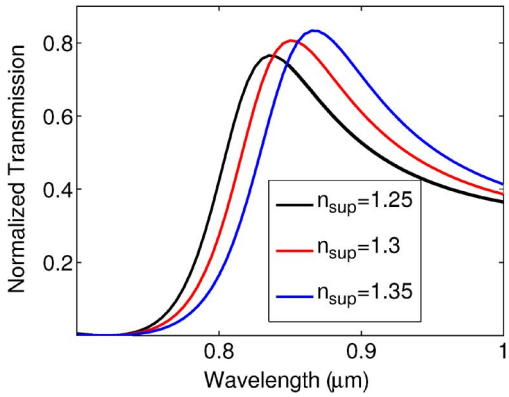

Fig. 3. Normalized transmission for a change in the refractive index of superstrate (n_{sup}) and geometrical features of $\Lambda = 450$ nm, $t = 160$, and $\rho = 0.3114$.

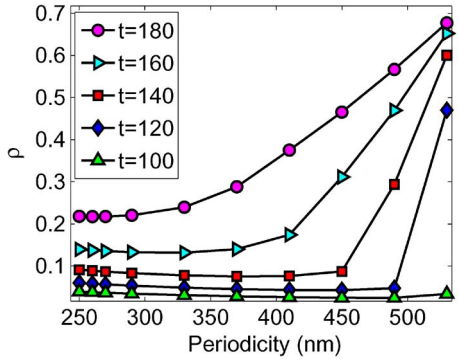

Fig. 4. Duty cycle (ρ) versus period (Λ) for different values of thickness (t) in nanometers to tune the resonance wavelength at 850 nm.

biasing our decision to wavelength-based effects, as discussed before. Our choice to fix the resonance wavelength is rooted in practice, where a sensor is often designed and optimized around a preferred wavelength due to practical constraints.

3.1. Fixing the Resonance Wavelength at 850 nm

We showed in Fig. 2(a)–(c) that λ_P is an increasing function of Λ and t and a decreasing function of ρ. Therefore, it is possible to fix λ_P at 850 nm by properly tuning these parameters. Essentially, $\lambda_P = 850$ nm is a 2-D subspace of the 3-D space of the structural parameters of the plasmonic grating sensor. For easier visualization, we slice this 2-D curved plane at various values of the thickness t and plot the intersections in Fig. 4. For example, the curve marked by $t = 180$ in Fig. 4 is the locus of points where $t = 180$ nm and $\lambda_P = 850$ nm. We show that it is possible to tune the resonance wavelength at 850 nm for a wide range of the structural parameters of the plasmonic grating structure. For large values of t, large variations in ρ are required to compensate for changes in Λ to fix λ_P. However, for small values of t, especially in regions with lower values of Λ, a small change in ρ is needed to compensate for large variations in Λ, as can be seen in Fig. 4.

The shape of the transmission spectrum varies considerably across all these possible design points. The considerable variation in the shape of the transmission spectra translates into different values of the LOD metric, as will be explained in detail in the next subsection. At this point, we find it instructive to show the shape of the transmission spectrum of some of the design points (from Fig. 4) in Fig. 5. The transmission spectra in Fig. 5(a)–(e) correspond to $t = 100$ nm, 120 nm, 140 nm, 160 nm, and 180 nm, respectively. The corresponding duty cycle ρ can be found in Fig. 4. We caution the reader that the results in Fig. 5 should not be compared with those of Fig. 2(a)–(c), since the constraint of

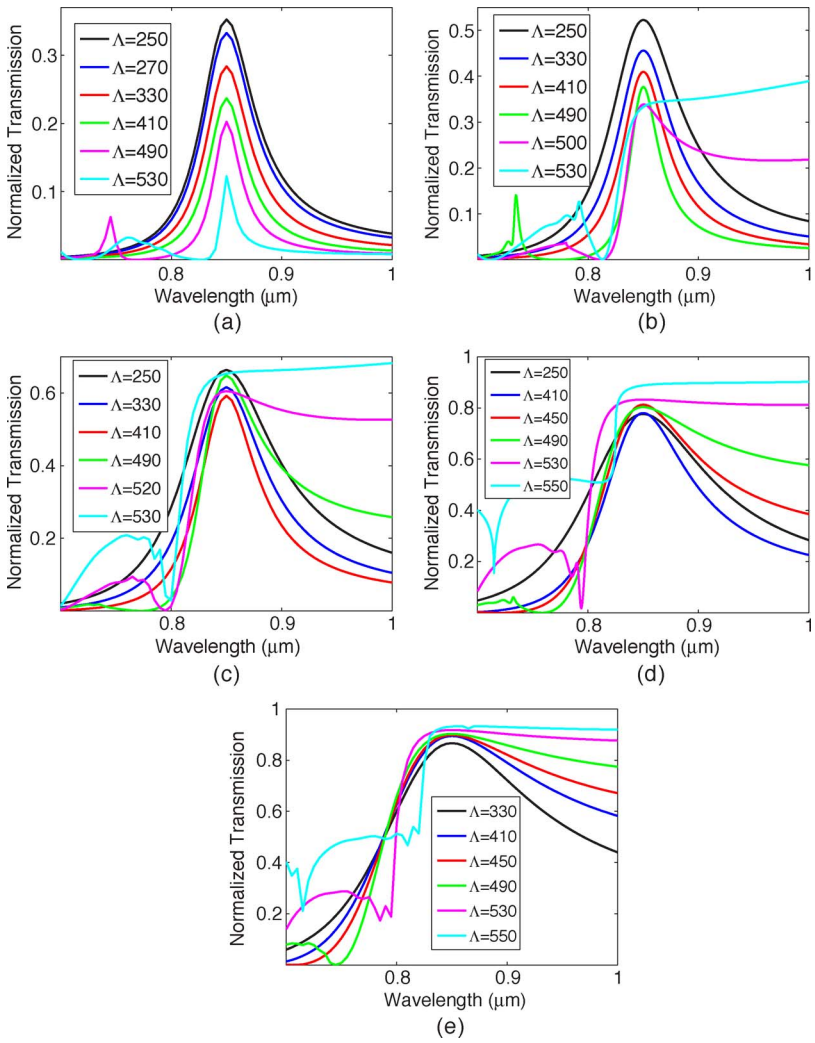

Fig. 5. Enhanced transmission spectrum for different values of period, duty cycle, and thicknesses of (a) 100 nm, (b) 120 nm, (c) 140 nm, (d) 160 nm, and (e) 180 nm.

$\lambda_P = 850$ nm is applied in generating the plots in Fig. 5. It is immediately clear that a metric solely based on the value of the FWHM will strongly favor smaller values of t, ignoring the fact that the transmission peak is quite short in this parameter range. The variation of the FWHM is plotted across the design parameter in Fig. 6. For the thickness value of 100 nm, it is possible to define FWHM for almost all considered values of Λ (except $\Lambda = 550$ nm), and the trend is decreasing by increasing the value of the period. However, for the other values of the thickness considered here, the strong asymmetry of the spectral transmission shape for period values higher than 430 nm prevents us from properly identifying (or in some cases even defining) the FWHM in the spectral range of our studies. The above discussion clearly illustrates the need for a proper metric which incorporates the FWHM, the peak value, as well as other spectral shape features. This issue will be discussed in the next subsection.

3.2. LOD Based on the CRB

In the plasmonic grating sensors discussed in this paper, the relevant spectral features which are used for sensing are the resonant peaks, where the sensing signature is a spectral shift of these resonant features caused by a change in the refractive index of the analyte in the superstrate. We argued that the proper metric to be used for the optimization of our plasmonic sensor is the LOD for

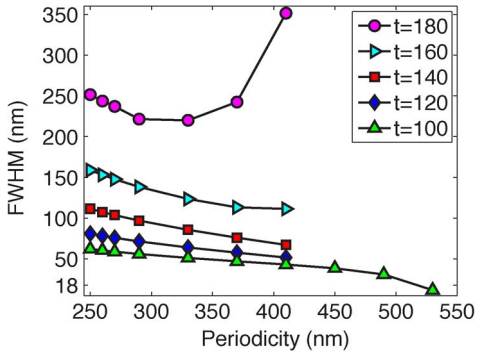

Fig. 6. FWHM versus period for different values of the grating thickness with a tuned resonance wavelength at 850 nm.

a wavelength shift in the spectral features. Our definition of the LOD is based on the CRB that determines the theoretical lower-bound on the estimation uncertainty of the spectral shift [11]. In this paper, we follow the usual definition of LOD which is proportional to $\sigma_\lambda / s_\lambda$, where σ_λ and s_λ are the standard deviation of the measured parameter and the sensor sensitivity, respectively. The variance in the estimation of a spectral shift in the presence of photon noise with Poisson statistics for a continuously sampled signal is given by (see Appendix I)

$$var(\Delta\lambda) \geq \frac{\delta\lambda}{\mathrm{SNR}^2} \left(\int_{\mathcal{W}} \frac{(dT(\lambda)/d\lambda)^2}{T(\lambda)} d\lambda \right)^{-1}. \tag{2}$$

$T(\lambda)$ is the normalized transmission spectrum, SNR is the signal-to-noise ratio, $\sigma_\lambda^2 = var(\Delta\lambda)$, $\mathcal{W}$ is the spectral width of the sampled signal, and $\delta\lambda$ is the sampling resolution. The integral is taken over $\mathcal{W}$, whose size is determined by the spectral range of the detector.

We also remind that s_λ is virtually constant over the sensor design parameter range. Therefore, in order to optimize the performance of the sensor, it is sufficient to minimize $var(\Delta\lambda)$ (or σ_λ) over the design space. We note that the integral in (2) is dominated by those spectral features which have large slopes (large derivatives) and have large amplitudes. Since σ_λ is inversely proportional to the integral, large slopes and large amplitudes are the preferred features to minimize the LOD. For regular symmetric Lorentzian spectral peaks, large slopes and large amplitudes are equivalent to tall peaks with narrow FWHM, in agreement with common intuition. Similar to Karl *et al.* [11] and Hastings [10], we have assumed that photon noise is the dominant noise source. This is a reasonable choice for scientific grade CCD-based spectrometers where the CCD sensors are cooled to reduce thermal noise, as long as the exposure time is sufficiently long to achieve photon-noise limited operation [12].

At this point, we can readily apply (2) to the normalized transmission spectra of Fig. 5 over an appropriate spectral range of $\mathcal{W}$ and numerically evaluate the optimum structural parameters which minimize σ_λ. Although some insightful analytical simplifications are possible for (2), as presented in Appendix II, full numerical evaluation is necessary for proper optimization. In Fig. 7, we present the numerical evaluation of the standard deviation in the measurement of the wavelength shift σ_λ over the design parameter space. The vertical axis is the normalized standard deviation $\gamma_\lambda = (\mathrm{SNR}^2/\delta\lambda)\sigma_\lambda^2$. γ_λ is plotted as a function of the period for different values of the thickness at each line corresponding to $t = 100$ nm, 120 nm, 140 nm, 160 nm, and 180 nm. We use similar structural parameters as those presented in Figs. 4 and 6. The values of the duty cycle and FWHM at each point can be determined from Fig. 4. In order to perform the numerical integration in (2), we choose a wavelength range $\mathcal{W}$ of 700 nm to 1000 nm. From Fig. 7, it is clear that a grating with a thickness of $t = 160$ nm and period $\Lambda = 530$ nm corresponding to a duty cycle of $\rho = 0.14$ provides the lowest LOD for our plasmonic grating sensor. The corresponding spectral transmission curve in

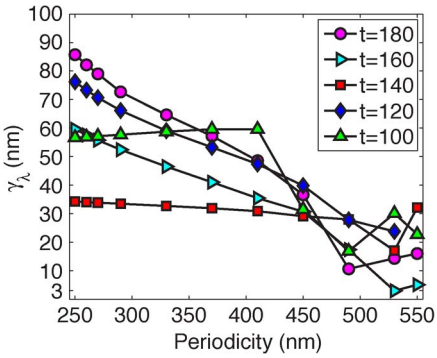

Fig. 7. Variance in estimation of spectral shift versus period for different thicknesses.

Fig. 5(d) is the highly asymmetric one with a step-like feature. The large intensity slope $dT/d\lambda$ near 850 nm is responsible for the low value of LOD at this point in the design parameter space. By comparing Figs. 6 and 7, we conclude that the structural parameters which result in the lowest LOD are not the narrowest in FWHM of the transmission spectrum. It is the intensity slope, and not the FWHM, which is responsible for low LOD values. In fact, the smallest LOD values in our structures belong to a region in our parameter space where the FWHM cannot even be defined or is infinitely large. We note that the common intuition that identifies the narrower FWHM with the lower LOD is merely based on the Lorentzian-like resonances where some of the spectral features in our grating plasmonic sensor are far from Lorentzian.

In practice, the resolution of the spectrometer and the SNR determine the theoretically minimum detectable shift in the value of the refractive index of the analyte. For example, in order to be able to detect a minimum shift in the refractive index of $\delta n \approx 10^{-5}$, we should be able to detect at least a spectral shift of $S_\lambda \delta n \approx 4.5 \times 10^{-3}$ nm; therefore $\sigma_\lambda \leq 4.5 \times 10^{-3}$ nm. The minimum detectable wavelength shift is given by the geometrical mean of the spectrometer resolution and the value of γ_λ reported in Fig. 7, divided by the SNR

$$\sigma_\lambda = \frac{\sqrt{\delta\lambda \times \gamma_\lambda}}{\text{SNR}}. \tag{3}$$

If the resolution of the spectrometer is $\delta\lambda \approx 0.1$ nm and $\gamma_\lambda \approx 3$ nm, we will need SNR ≥ 120. We remind that SNR is defined based on the number of photons incident on the grating in the wavelength interval of $\delta\lambda$ and its relationship to the total SNR in presented in Appendix I.

4. Conclusion

We conclude that the optimal design based on the LOD metric for our plasmonic grating sensor results in highly asymmetric step-like spectral features that do not conform to the common intuition of tall narrow Lorentzian peaks. Although we have chosen a specific design for our case study for water-monitoring applications, much of our observations should be applicable to similar plasmonic grating sensor designs. Our study over a wide range of the structural parameters of the grating at fixed interrogation wavelength of 850 nm shows a general preference for larger values of period, hence easier fabrication. Although LOD was lowest for a grating thickness of 160 nm, we observe comparable results over a wide range of thickness values from 120 nm to 160 nm. However, a thickness value of 160 nm is also associated with a larger value of the duty cycle, making the fabrication easier. Therefore, the best design based on the LOD metric is gold stripes of 160 nm thickness and 456 nm width, where the stripes are separated by 74 nm.

We would like to emphasize that the strong transmission spectral asymmetry observed in our gratings results in rather different observations from what was previously reported by Hastings [10]. Specifically, we have shown that FWHM and transmission peak can be misleading metrics, and proper analysis based on LOD can result in non-intuitive optimal designs.

Appendix I
CRB in the Presence of Poisson Noise

In this paper, we adopt the derivation of the CRB for the LOD as presented by Karl *et al.* [11]. Hastings [10] recently applied this derivation to the study of prism-based plasmonic sensors with Lorentzian spectral features. The variance in the estimation of a spectral shift in the presence of noise with Poisson statistics for a signal sampled at N wavelengths λ_i is given by

$$var(\Delta\lambda) \geq \left(\sum_{i=1}^{N} P_i \frac{\left[\frac{dT}{d\lambda}\right]^2_{\lambda_i - \Delta\lambda}}{T(\lambda_i - \Delta\lambda)} \right)^{-1}$$

where P_i is the total number of incident photons at the sampled wavelength λ_i. Since we are interested in the core relationships in a model independent way, we make the simplifying assumption that the number of incident photons P_i is constant across the interrogation region $\mathcal{W}$. However, this analysis can be easily extended by including the spectral dependence of the light source by using nonuniform P_i. Alternatively, a renormalization of $T(\lambda)$ (keeping P_i constant) can be used as a reasonable approximation to incorporate the spectral dependence of the light source (and the detector efficiency). The standard deviation of the incident photon number (shot noise) at each sampled point is $\sqrt{P_i}$. Therefore, the signal-to-shot-noise ratio is given by

$$\text{SNR} = \frac{\text{Signal}}{\text{Noise}} = \frac{P_i}{\sqrt{P_i}} = \sqrt{P_i}.$$

For a signal which is uniformly sampled in equal intervals of wavelength $\delta\lambda$, for sufficiently small $\delta\lambda$, the discrete sum can be approximated with an integral over the interrogation region $\mathcal{W}$, where $\mathcal{W} = N\delta\lambda$. We can write (for small $\Delta\lambda$)

$$var(\Delta\lambda) \geq \frac{\delta\lambda}{\text{SNR}}^2 \left(\int_{\mathcal{W}} \frac{(dT(\lambda)/d\lambda)^2}{T(\lambda)} d\lambda \right)^{-1}.$$

One can also use the total SNR where $\text{SNR}_{\text{total}} = \sqrt{N} \times \text{SNR}$. In practice, $\delta\lambda$ can be regarded as the resolution of the spectrometer.

Appendix II
CRB in the Presence of Poisson Noise

We would like to point out that the asymmetric profile of the enhanced transmission spectrum can be fitted to a Fano resonance [13], [14]. The Fano-resonance is of the form [13]

$$T(\lambda) = \frac{A}{1+q^2} \frac{\left(q\frac{w_0}{2} + \lambda - \lambda_0\right)^2}{\left(\frac{w_0}{2}\right)^2 + (\lambda - \lambda_0)^2}. \quad (4)$$

The transmission spectrum peaks at $\lambda_P = \lambda_0 + w_0/(2q)$, and its peak value is given by A. The FWHM of the transmission spectrum is also given by $w_0(q^2+1)/(q^2-1)$. The Fano-resonance becomes Lorentzian in the limit of $q \to \infty$ and the FWHM is only applicable for $q > 1$ in our fits. The values of the q parameter close to or smaller than unity correspond to the highly asymmetric step-like transmission spectra of Fig. 5 for which the FWHM cannot be properly defined. The quality of the fit remains excellent over the entire range of our studied parameter space. However, the fit cannot reproduce the spectral bumps in Fig. 5 that appear at wavelengths shorter than 800 nm for a few of the highly asymmetric peak features. We can now use (4) in (2) to estimate the LOD for the plasmonic grating sensor. For most of the design parameter space, the range of integration in (2) can be extended to $\lambda \in (-\infty, \infty)$. Although the validity range of the Fano-resonance fit is limited, the integrand is negligible, except in the vicinity of the spectral peak. As long as the wavelength

interrogation range $\mathcal{W}$ is large enough, it can be reliably replaced with the entire real line in the integral. However, we have observed that this approximation fails for highly asymmetric spectral features. Considerable analytical simplification is obtained by using the above approximation, and we can write

$$\sigma_\lambda^2 = var(\Delta\lambda) \geq \frac{\delta\lambda}{\mathrm{SNR}^2} \frac{w_0(q^2+1)}{A\pi(q^2+3)}. \tag{5}$$

Alternatively, we can express (5) in terms of the FWHM of the transmission resonance peak as

$$\sigma_\lambda^2 = var(\Delta\lambda) \geq \frac{\delta\lambda \times \mathrm{FWHM}}{\pi A \times \mathrm{SNR}^2} \left(\frac{q^2-1}{q^2+3}\right). \tag{6}$$

The scaling of σ_λ with the square root of the FWHM was previously reported in studies of other configurations of plasmonic sensors by Homola *et al.* [15] and Hastings [10]. Similarly, larger values of SNR and higher sampling resolution $\delta\lambda$ (spectrometer resolution) lower the LOD bound. Of course, it is understood that (6) fails to account for the behavior of the highly asymmetric transmission features whose q parameter is less than or only slightly larger than unity and is most accurate for large values of q parameter. We previously argued that the LOD metric in (2) favors spectral features with large intensity slope $dT/d\lambda$. In fact, the largest slopes in Fig. 5 are from those curves that cannot be described by the approximations used in the derivation of (6). Therefore, although (6) is insightful, it cannot be used for the LOD optimization of the plasmonic sensor.

References

[1] T. W. Ebbesen, H. J. Lezec, H. F. Ghaemi, T. Thio, and P. A. Wolff, "Extraordinary optical transmission through subwavelength hole array," *Nature*, vol. 391, no. 6668, pp. 667–669, Feb. 1998.

[2] C. Genet and T. W. Ebbesen, "Light in tiny holes," *Nature*, vol. 445, no. 7123, pp. 39–46, Jan. 2007.

[3] J. A. Porto, F. J. Garcıa-Vidal, and J. B. Pendry, "Transmission resonances on metallic gratings with very narrow slits," *Phys. Rev. Lett.*, vol. 83, no. 14, pp. 2845–2848, Oct. 1999.

[4] X. Shou, A. Agrawal, and A. Nahata, "Role of metal thickness on the enhanced transmission properties of a periodic array of subwavelength apertures," *Opt. Express*, vol. 13, no. 24, pp. 9834–9840, Nov. 2005.

[5] [Online]. Available: www.comsol.com

[6] K. M. Gundu, M. Brio, and J. V. Moloney, "A mixed high-order vector finite element method for waveguides: Convergence and spurious mode studies," *Int. J. Numer. Model.: Electron. Netw., Devices Fields*, vol. 18, no. 5, pp. 351–364, Sep./Oct. 2005.

[7] K. M. Gundu and A. Mafi, *Reliable computation of scattering from metallic binary gratings using modal methods*.

[8] P. B. Johnson and R. W. Christy, "Optical constants of noble metals," *Phys. Rev. B, Condens. Matter*, vol. 6, no. 12, pp. 4370–4379, Dec. 1972.

[9] S. A. Darmanyan and A. V. Zayast, "Light tunneling via resonant surface plasmon polariton states and enhanced transmission of periodically nanostructured metal films: An analytical study," *Phys. Rev. B, Condens. Matter*, vol. 67, no. 3, p. 035 424, Jan. 2003.

[10] J. T. Hastings, "Optimizing surface-plasmon sensors for limit of detection based on Cramer–Rao bound," *IEEE Sensors J.*, vol. 8, no. 2, pp. 170–175, Feb. 2008.

[11] W. C. Karl and H. Pien, "High-resolution biosensor spectral peak shift estimation," *IEEE Trans. Signal Process.*, vol. 53, no. 12, pp. 4631–4639, Dec. 2005.

[12] [Online]. Available: http://learn.hamamatsu.com/articles/ccdsnr.html

[13] U. Fano, "Effect of configuration interaction on intensities and phase shift," *Phys. Rev.*, vol. 124, no. 6, pp. 1866–1878, Dec. 1961.

[14] C. Genet, M. P. van Exter, and J. P. Woerdman, "Fano-type interpretation of red shifts and red tails in hole array transmission spectra," *Opt. Commun.*, vol. 225, no. 4–6, pp. 331–336, Oct. 2003.

[15] R. Slavik, J. Homola, and H. Vaisocherova, "Advanced biosensing using simultaneous excitation of short and long range surface plasmons," *Meas. Sci. Technol.*, vol. 17, no. 4, pp. 932–938, Apr. 2006.